https://doi.org/10.5194/nhess-2022-244
Preprint. Discussion started: 18 October 2022

Natural Hazards and Earth System Sciences
Open Access
Discussions

Hydrological Drought forecasting under changing environment in Luanhe River basin

Min Li[1,2], Mingfeng Zhang[2], Runxiang Cao[3], Yidi Sun[2], Xiyuan Deng[4,5],

[1] State Key Laboratory of Hydraulic Engineering Simulation and Safety， Tianjin University, Tianjin, China;

[2] College of Hydraulic Science and Engineering, Yangzhou University, JiangSu, China;

[3]College of Water Resources, North China University of Water Resources and Electric Power, Zhengzhou 450046, China;

[4]Nanjing Hydraulic Research Institute, Nanjing, 210029, China; [5]State Key Laboratory of Hydrology-Water Resources and Hydraulic Engineering，Nanjing, 210029, China

Correspondence to: Min Li (limintju@126.com); Xiyuan Deng (xydeng@nhri.cn)

https://doi.org/10.5194/nhess-2022-244
Preprint. Discussion started: 18 October 2022

Natural Hazards and Earth System Sciences
Discussions

Abstract: Hydrological drought forecasting can mitigate the socio-economic and ecological impacts of drought. It is an important disaster reduction strategy to forecast the occurrence of hydrological drought according to the forecasting system. In this paper, the conditional distribution model with human activity factor as exogenous variable was constructed to forecast the hydrological drought based on meteorological drought, and then compared with the traditional normal distribution model and conditional distribution model. The results show that the runoff series of Luanhe River Basin from 1961 to 2010 was non-stationary. For the traditional conditional probability models, the transition probabilities of drought were affected by SPI time scales and forecasting periods. In order to analyze the impact of human activities on hydrological drought, we constructed the human activity factor based on the method of restoration. Subsequently, the conditional distribution models involving human index were constructed and the influence of human activities on drought transition probability was analyzed. With the increase of human index (*HI*) value, hydrological droughts tend to transition to more severe droughts. Finally, a scoring mechanism was applied to evaluate the performance of three drought forecasting models. According to the scores of the three drought forecasting models, the conditional distribution model involving of human activity factor can further improve the forecasting accuracy of drought in Luanhe River Basin.
Keyword: Changing environment; Drought forecasting; Human activity factor; Luanhe River basin

1 Introduction

Typically, meteorological drought is regarded as the beginning of a drought event; after the occurrence of meteorological drought, other drought phenomena occur, such as hydrological drought (Miriam et al., 2018; Fuentes et al., 2022; Wang et al., 2021). However, there is a delay period from meteorological drought to hydrological drought (Ding et al., 2021; Xu et al., 2019). Therefore, the occurrence of hydrological drought can be forecasted according to meteorological drought monitoring. Accurate hydrological forecast information is beneficial to reduce the losses caused by hydrological drought. (Behzad and Hamid, 2019; Melanie et al., 2018).

Statistical technology is an effective prediction method that has been widely used in drought forecasting in recent years (Bonaccorso et al., 2015). Focusing on statistical techniques, several mathematical statistical models have been applied to forecast drought, such as neural network models (Mehdi et al., 2016; Maryam et al., 2017; Ahnadi et al., 2011), time series modelling (Mohammad et al., 2020; Natsagdorj et al., 2021; Stojković et al., 2020) and hybrid models (Alquraish et al., 2021; Abbasi et al., 2021; Bagher et al., 2013). Some scholars focus on the transition probability of the drought class, which is mainly based on a certain drought index, such as the standardized precipitation index (SPI), the Palmer drought severity index (PDSI) or the standardized runoff index (SRI) (McKee, 1993; Palmer, 1965; Shukla, 2008). Mallya et al. (2013) assessed a drought probability based on a hidden Markov model (HMM) and then analysed the drought characteristics of Indiana. Moreira et al. (2013) calculated the SPI time series in the Alentejo area from 1932 to 1999, and then loglinear models were fitted to assess drought class transition probabilities. Based on the Multivariate Standardized Precipitation Index (MSPI), Aghelpour and Varshavian (2021) proposed the hybrid model to forecast the hydrological drought in Iran, which significantly improved the forecasting accuracy. Majid et al. (2019) used Archimedean copulas to model the relationship between the SPI and standardized hydrological drought index (SHDI), and the results indicated that hydrological drought class forecasting in the coming month is promising with less than 10% error.

Considering the impact of the changing environment, Bonaccorso et al. (2015) calculated SPI values under distinct time scales and analysed the conditional probabilities from the current SPI values to the future SPI classes. Ren et al. (2017) found that a model using large-scale climatic indices as covariates can improve the accuracy of meteorological drought forecasting in the Luanhe River Basin. Although some progress has been made in the study of drought forecasting, there are few studies considering the impact of changing environments.

To date, some studies have found nonstationary characteristics in the hydrological series of the Luanhe River Basin under changes in the environment (Wang et al., 2018; Li et al., 2015; Wang et al., 2016). The nonstationarity of hydrological series may lead to the nonstationarity of the relationship between hydrological series (for example, precipitation and runoff series), and traditional drought prediction methods are no longer applicable (Wang et al.,2022; Dixit et al.,2022; Muhammad et al.,2020; Zhao et al.,2018; Charles, 2017; Carmelo and Jü

https://doi.org/10.5194/nhess-2022-244
Preprint. Discussion started: 18 October 2022

rgen, 2018).

The research contents of this paper are as follows: (1) The SPI series and SRI series are calculated according to the monthly rainfall and runoff data of the Luanhe River Basin from 1961 to 2010. (2) A multivariate normal distribution model (Model 1), conditional distribution model (Model 2) and conditional distribution model with the human index (*HI*) as an exogenous variable (Model 3) were constructed to calculate the transition probabilities from current SPI classes or values to future SRI classes. (3) A scoring mechanism was applied to the evaluation of the three probability models.

In addition to the introduction, this paper also contains the following sections. Section 2 introduces the study area and data. Section 3 briefly describes the methods used in the research. Section 4 introduces the model construction and calculation results and analyses the results. Section 5 presents the prospects.

2 Study area and data

The Luanhe River Basin, located in the subtropical monsoon region, covers an area of approximately 33700 square kilometres. Its geographical location is shown in Figure 1. Due to the influence of geographical location and topography, the annual average north-south temperature difference in the basin is 11.5 °C, and the annual rainfall distribution is uneven. Less rain in spring and winter makes the area prone to meteorological drought and hydrological drought, while there is relatively more rainfall in summer. The average rainfall in summer is approximately 200-560 mm, resulting in highly variable annual runoff of the basin. The concentrated rainfall in summer has also become one of the remarkable features of the climate in this area. In recent years, the precipitation and inflow of the Luanhe River Basin have gradually decreased, the water level of the Panjiakou Reservoir in the lower reaches of the basin has decreased, the runoff has also decreased, and the frequency of meteorological drought and hydrological drought has significantly increased. Especially after entering the 21st century, the river basin has exhibited the phenomenon of continuous drought and even extreme drought. With the change in the global climate and the impact of

https://doi.org/10.5194/nhess-2022-244
Preprint. Discussion started: 18 October 2022

Natural Hazards and Earth System Sciences
Open Access
Discussions

human activities on the basin environment, drought disasters in the Luanhe River Basin occur frequently, causing significant social and economic losses.

In this paper, the monthly rainfall data from 26 stations in the Luanhe River Basin from 1961 to 2010 are provided by the Hebei Provincial Hydrology and Water Resources Investigation Bureau. The average monthly rainfall data of the area are obtained by spatial interpolation. The runoff data from 1961 to 2010 come from the inflow runoff series of the Panjiakou Reservoir. The SPI and SRI can be calculated for 1-month, 3-month, 6-month, and 12-month time scales to characterize meteorological drought and hydrological drought based on these data.

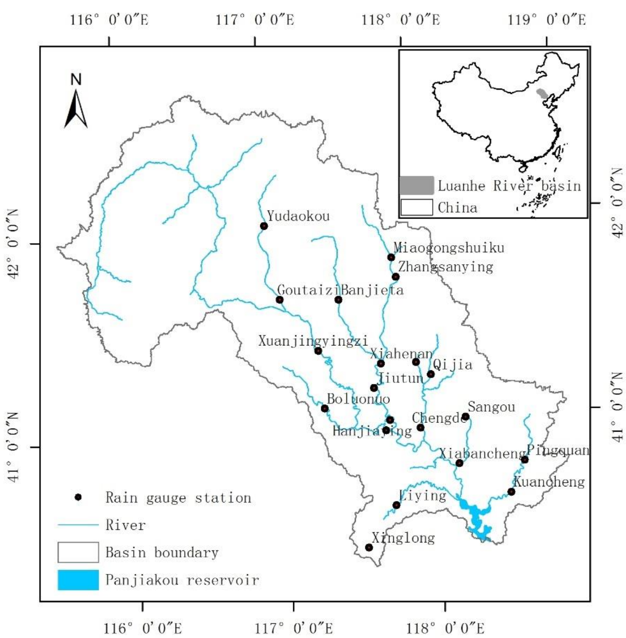

Figure 1 The geographical location of the Luanhe River Basin

3 Methods

3.1 Nonstationarity test method

In the case of environmental changes, nonstationarity may occur in hydrological series. The Pettitt test, as one of the important methods to test whether there is nonstationarity in time series, can identify whether there are change points in the

https://doi.org/10.5194/nhess-2022-244
Preprint. Discussion started: 18 October 2022

sample series (Malede et al., 2022). Assuming that the sample sequence is $x=(x_1,x_2,\cdots x_n)$, the formula is as follows:

$$U_{t,n}=U_{t-1,n}+\sum_{i=1}^{n}\operatorname{sgn}(x_t-x_i)\quad(t=2,3,\cdots n)t_0 \tag{1}$$

$$\operatorname{sgn}(x_t-x_i)=\begin{cases}1 & x_t-x_i>0\\ 0 & x_t-x_i=0\\ \text{-1} & x_t-x_i=0\end{cases} \tag{2}$$

where $U_{t,n}$ is the test statistic, which indicates the cumulative number of the values at time t greater than or less than the values at time i. In addition, if $K_{t0,n}$ satisfies:

$$K_{t0,n}=\max\left|U_{t,n}\right|\quad(\text{t=1,2,}\cdots\text{,n}) \tag{3}$$

Then, t_0 is considered to be the change point, and the cumulative probability of possible change is determined by $K_{t0,n}$:

$$P_{t0,n}=2\exp\left(-\frac{6K_{t0,n}^2}{n^3+n^2}\right) \tag{4}$$

Given the significance level $\alpha=0.05$, if $P_{t0,n}$ >0.95, it means that the point is a significant change point (Li et al., 2022; Koudahe et al., 2018). Furthermore, combined with the Mann-Kendall test, the trend characteristics of the sample series can be obtained (Linchao et al., 2018).

The sliding T test is a basic method commonly used in statistics. According to the mean and variance of the two sample sequences before and after the change points in the runoff time series, the two sample sequences are tested (Li et al., 2020):

$$t=\frac{\overline{x}_1-\overline{x}_2}{S\sqrt{\frac{1}{n_1}+\frac{1}{n_2}}} \tag{5}$$

$$S=\sqrt{\frac{(n_1-1)S_1^2+(n_2-1)S_2^2}{n_1+n_2-2}} \tag{6}$$

$$S_1^2=\frac{1}{n_1-1}\sum_{t=1}^{n_1}(x_t-\overline{x}_1)^2 \tag{7}$$

$$S_2^2=\frac{1}{n_2-1}\sum_{t=1}^{n_1+n_2}(x_t-\overline{x}_2)^2 \tag{8}$$

Here, assume that the change point is x_t, n_1 and n_2 represent the sample size before and after the change point, S_1^2 and S_2^2 represent the variance of the samples before and after the change point, respectively If the statistic t satisfies $t > t_\alpha$ as the significance level is $\alpha = 0.05$, the point can be considered the change point.

The Spearman correlation test can be applied to test the trend of time series, and the specific description refers to the article of Bishara and Hittner (2012).

3.2 Human activity index (*HI*)

The double cumulative curve method can test the nonstationarity of the bivariate correlation between rainfall series and runoff series, and the point where the underlying surface is significantly altered by human activities can be determined according to the position of the slope change of the curve. The linear regression relationship of the cumulative rainfall and runoff series can be calculated according to the following formula:

$$\sum x = k \sum y + b \tag{9}$$

Here, *x* is the runoff series; *y* is the rainfall series; *k* is the correlation coefficient of the regression equation; and *b* is the intercept of the regression equation.

Human activities are the main reason for the nonstationarity of the runoff series in the watershed, so the human activity index (*HI*) can be constructed to quantify the impact of human activities on runoff. Based on the linear regression relationship established between the accumulated precipitation and the accumulated runoff before the change point, the theoretical runoff sequence during the human activity period can be calculated from the measured precipitation sequence. SRI' represents the standardized runoff index value without human activity interference, and SRI represents the normalized runoff index value calculated based on the measured runoff sequence under the disturbance of human activities. The *HI* is obtained by subtracting the theoretical SRI' and the actual SRI, and the calculation formula is as follows:

$$HI = SRI' - SRI \tag{10}$$

When HI>0, it can be assumed that human activities exacerbate hydrological drought, HI<0 has the opposite effect, and HI=0, the watershed is considered undisturbed by human activities.

3.3 Multivariate normal distribution model

The SPI is one of the important indicators for evaluating meteorological drought in the basin, and the SRI is an important indicator for evaluating hydrological drought in the basin. According to the rainfall data and runoff data in the basin, the SPI and SRI at different time scales can be calculated. Table 1 provides the drought class classification and corresponding SPI values and SRI values (Kolachian and Saghafian, 2021).

Table 1 Drought class classification and corresponding SPI values and SRI values

SPI/SRI values	Class
> -0.99	Normal
-1.00 to -1.49	Moderate
-1.50 to -1.99	Severe
≤ -2.00	Extreme

As a traditional drought class forecasting model, the multivariate normal distribution model (Model 1) can forecast the future SRI class according to the current SPI class. Assuming that both the current SPI and SRI sequence satisfy a multivariable normal distribution, the joint probability density can be expressed as follows (Chang et al.,2022):

$$f_{Z_{v,\lambda}^{(k)}W_{v,\lambda+M}^{(k)}}(t,s)=\frac{1}{2\pi|\Sigma|}\cdot\exp\left(-\frac{1}{2}X^{T}\Sigma^{-1}X\right) \tag{11}$$

Here, $\sum$ is the covariance matrix, and $X=[t,s]^{T}$. The form of the covariance matrix is as follows:

$$\Sigma=\begin{bmatrix}1 & \mathrm{cov}\left[Z_{v,\lambda}^{(k)},W_{v,\lambda+M}^{(k)}\right]\\ \mathrm{cov}\left[Z_{v,\lambda}^{(k)},W_{v,\lambda+M}^{(k)}\right] & 1\end{bmatrix} \tag{12}$$

Furthermore, according to the joint probability density function of the SPI value $Z_{v,\lambda}^{(k)}$ at v year and month λ and the future M months SRI value $W_{v,\lambda+M}^{(k)}$, the analytical

https://doi.org/10.5194/nhess-2022-244
Preprint. Discussion started: 18 October 2022

formula of the transition probability of the future SRI drought class can be obtained (Zhang et al., 2017):

$$P\left[W_{v,\lambda+M}^{(k)} \in C_M\right] = \frac{\iint_{C_N C_M} f_{Z_{v,\lambda}^{(k)} W_{v,\lambda+M}^{(k)}}(t,s) \cdot dt \cdot ds}{\int_{C_N} f_{Z_{v,\lambda}^{(k)}}(t) \cdot dt} \tag{13}$$

where C_M represents the drought class and $f_{Z_{v,\lambda}^{(k)}}(t)$ represents the marginal density function of $Z_{v,\lambda}^{(k)}$ in the current λ month.

3.4 The conditional distribution model

The conditional distribution model (Model 2) proposed by Bonaccorso et al. (2015) is described as follows: when one group of sample data X obeys a normal distribution and satisfies $X \sim N(\mu_1, \Sigma_1)$, while another group of sample data Y also obeys a normal distribution, namely, $Y \sim N(\mu_2, \Sigma_2)$, then the total sequence can be written as follows:

$$B = \begin{bmatrix} X \\ Y \end{bmatrix} \begin{matrix} r \\ p-r \end{matrix} \sim N_p\left(\begin{bmatrix} \mu_1 \\ \mu_2 \end{bmatrix}, \begin{bmatrix} \Sigma_{11} & \Sigma_{12} \\ \Sigma_{21} & \Sigma_{22} \end{bmatrix}\right) \tag{14}$$

When sequence Y obeys a normal distribution, the distribution of sequence X under the Y condition still satisfies a normal distribution, namely, the distribution of $(X \mid Y)$ is as follows (Gong et al. 2021):

$$(X \mid Y) \sim N(\mu_3, \Sigma_3) \tag{15}$$

where μ_3 represents the expected value under the conditional distribution, and Σ_3 is the conditional covariance matrix:

$$\mu_3 = \mu_1 + \Sigma_{12}\Sigma_{22}^{-1}(y - \mu_2) \tag{16}$$

$$\Sigma_3 = \Sigma_{11} - \Sigma_{12}\Sigma_{22}^{-1}\Sigma_{21} \tag{17}$$

Assuming that the current SPI and the SRI sequence that transitioned from meteorological drought satisfy a binary normal distribution, then the probability of the transition to the future SRI drought class under the current SPI value can be deduced as follows (Ren et al., (2017)):

https://doi.org/10.5194/nhess-2022-244
Preprint. Discussion started: 18 October 2022

$$P\left[W_{v,\lambda+M} \in C_M \mid Z_{v,\lambda} = z_0\right] = \int_{C_{Mi}}^{C_{Ms}} \frac{1}{\sqrt{2\pi}\sigma_Z} e^{-\frac{1}{2}\left(\frac{x-\rho z_0}{1-\rho^2}\right)^2} dx \tag{18}$$

where $Z_{v,\lambda}$ represents the SPI value of the current month λ, $W_{v,\lambda+M}$ represents the SRI value of the $\lambda+M$ month, C_{Ms} and C_{Mi} are the upper and lower limits of the drought class C_M, and the correlation coefficient between the current SPI value and the future SRI value is ρ. Furthermore, the current SPI and future SRI can be expressed as the standard normal cumulative distribution function Φ:

$$P\left[W_{v,\lambda+M} \in C_M \mid Z_{v,\lambda} = z_0\right] = \Phi\left[\frac{C_{Ms} - \rho \bullet z_0}{1-\rho^2}\right] - \Phi\left[\frac{C_{Mi} - \rho \bullet z_0}{1-\rho^2}\right] \tag{19}$$

The calculation of the correlation coefficient ρ is as follows:

$$\rho = \frac{\operatorname{cov}[Z_{v,\lambda}^{(k)}, W_{v,\lambda+M}^{(k)}]}{\sqrt{\operatorname{var}(Z_{v,\lambda}^{(k)})\operatorname{var}(W_{v,\lambda+M}^{(k)})}} \tag{20}$$

K represents the time scale of the drought index. Assuming that the cumulative rainfall Y and runoff X satisfy a normal distribution, then after the standardization process, the SPI value $Z_{v,\lambda}^{(k)}$ corresponding to cumulative rainfall Y and SRI value $W_{v,\lambda+M}$ corresponding to runoff X obey the standard normal distribution (Wu, 2019), namely:

$$\operatorname{var}(Z_{v,\lambda}^{(k)}) = \operatorname{var}(W_{v,\lambda+M}^{(k)}) = 1 \tag{21}$$

$\operatorname{cov}[Z_{v,\lambda}^{(k)}, W_{v,\lambda+M}^{(k)}]$ represents the covariance between the current SPI and the Sri value with a forecast period of M months. The calculation is as follows:

$$\operatorname{cov}[Z_{v,\lambda}^{(k)}, W_{v,\lambda+M}^{(k)}] = \frac{1}{\sqrt{\sum_{i=0}^{k-1}\sigma_{\lambda+M-i}^2 \sum_{j=0}^{k-1}\sigma_{\lambda-j}^2}} \cdot \sum_{i=0}^{k-1}\sum_{j=0}^{k-1}\operatorname{cov}\left[X_{v,\lambda+M-j}, Y_{v,\lambda-i}\right] \tag{22}$$

3.5 The conditional distribution model involving *HI* as an exogenous variable

According to the above conditional probability model, when considering *HI* as an exogenous variable, the model (Model 3) can be extended as follows:

https://doi.org/10.5194/nhess-2022-244
Preprint. Discussion started: 18 October 2022

Natural Hazards and Earth System Sciences
Open Access
EGU
Discussions

$$P\left[W_{v,\lambda+M} \in C_M \mid Z_{v,\lambda} = z_0, H_{v,\lambda} = h_0\right] = \int_{C_{Mi}}^{C_{Ms}} \frac{1}{\sqrt{2\pi}\sigma_z} e^{-\frac{1}{2}\left(\frac{x-\mu_z}{\sigma_z}\right)^2} dx \tag{23}$$

$$\mu_z = E\left[W_{v,\lambda+M} \mid Z_{v,\lambda}, H_{v,\lambda}\right] = \Sigma'_{12}(\Sigma'_{22})^{-1}\begin{bmatrix} z_0 \\ h_0 \end{bmatrix} \tag{24}$$

$$\sigma_z^2 = \mathrm{var}\left[W_{v,\lambda+M} \mid Z_{v,\lambda}, H_{v,\lambda}\right] = 1 - \Sigma'_{12}(\Sigma'_{22})^{-1}\Sigma'_{21} \tag{25}$$

Where:

$$\Sigma'_{12} = \left[\mathrm{cov}(W_{v,\lambda+M}, Z_{v,\lambda}) \ \ \mathrm{cov}(W_{v,\lambda+M}, H_{v,\lambda})\right] \tag{26}$$

$$\Sigma'_{22} = \begin{bmatrix} 1 & \mathrm{cov}(Z_{v,\lambda}, H_{v,\lambda}) \\ \mathrm{cov}(H_{v,\lambda}, Z_{v,\lambda}) & 1 \end{bmatrix} \tag{27}$$

$$\Sigma'_{21} = (\Sigma'_{12})^T \tag{28}$$

4 Results and discussion

4.1 Nonstationarity analysis

In this paper, the area average monthly rainfall data of the Luanhe River Basin from 1961 to 2010 are obtained by spatial interpolation. The runoff data come from the inflow runoff series of the Panjiakou Reservoir. Given the significance level $\alpha = 0.05$, the nonstationarity test results are shown in Figure (2).

Figure 2 (a) shows that the years of possible runoff change were 1979, 1996, 1997, 1998, and 1999. The P values in 1979 and 1998 were infinitely close to 1, which were considered to be extremely significant runoff change points. Among all the possible points satisfying $t > t_\alpha$, there are two maximum points (Figure 2 (b)), namely, 1979 and 1998, which are considered to be possible runoff change points. The final change point needs to be judged based on the actual situation of the watershed.

https://doi.org/10.5194/nhess-2022-244
Preprint. Discussion started: 18 October 2022

Natural Hazards and Earth System Sciences
Discussions

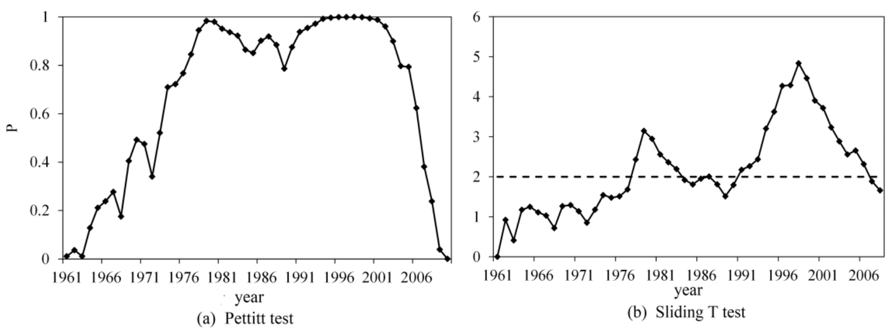

Figure (2) The change points of the runoff series

The results of the Spearman correlation test (Table 2) indicate that the runoff series showed an upwards trend before 1979, but the trend was not significant. However, there was a significant downwards trend in the series after 1979. In general, the runoff series showed a significant downwards trend.

Table 2. Spearman correlation test results of runoff series trend

Runoff series	statistic t	Critical value t_{α}
The whole series	-3.471	±2.009
Serie before 1979	0.691	±2.009
Serie after 1979	-2.292	±2.009

In addition, according to historical records, there were no extreme rainstorm events recorded during 1979. It can be inferred that the cause of the sudden change in annual runoff in 1979 was not the formation of heavy rainstorms in the previous period or the same period. Since the start of 1979, the underlying surface conditions of the basin have undergone large changes due to human activities, so it is determined that 1979 is the change point of the runoff sequence in the basin. Therefore, 1979 was finally determined as the change point of the runoff sequence of the Luanhe basin from 1961 to 2010. This conclusion is consistent with Li et al. (2015) and Wang et al. (2015).

4.2 Transition probabilities from current SPI values to future SRI classes

According to the normality test results of rainfall and runoff series, it is reasonable to apply the conditional distribution model. To analyse the influence of different time scales of SPI on the transition probabilities, using the forecast period as

https://doi.org/10.5194/nhess-2022-244
Preprint. Discussion started: 18 October 2022

one month and the time scales of SPI on 1-month, 3-month, 6-month and 12-month as examples, the probabilities of converting SPI values to SRI classes were calculated (Figure (3)).

As shown in Figure (3), when meteorological drought is categorised as extreme drought, the probability of maintaining the SRI class in the extreme drought state is greater as the time scale of the SPI increases. As the SPI is a 12-month time scale, the drought transition probability is close to 1. However, while the time scale is small, the response of the future SRI value to rainfall is faster, so the probability of tending to the normal state is greater. In the future, the response of the SRI value to rainfall is relatively fast, so it is more likely to tend to a normal state.

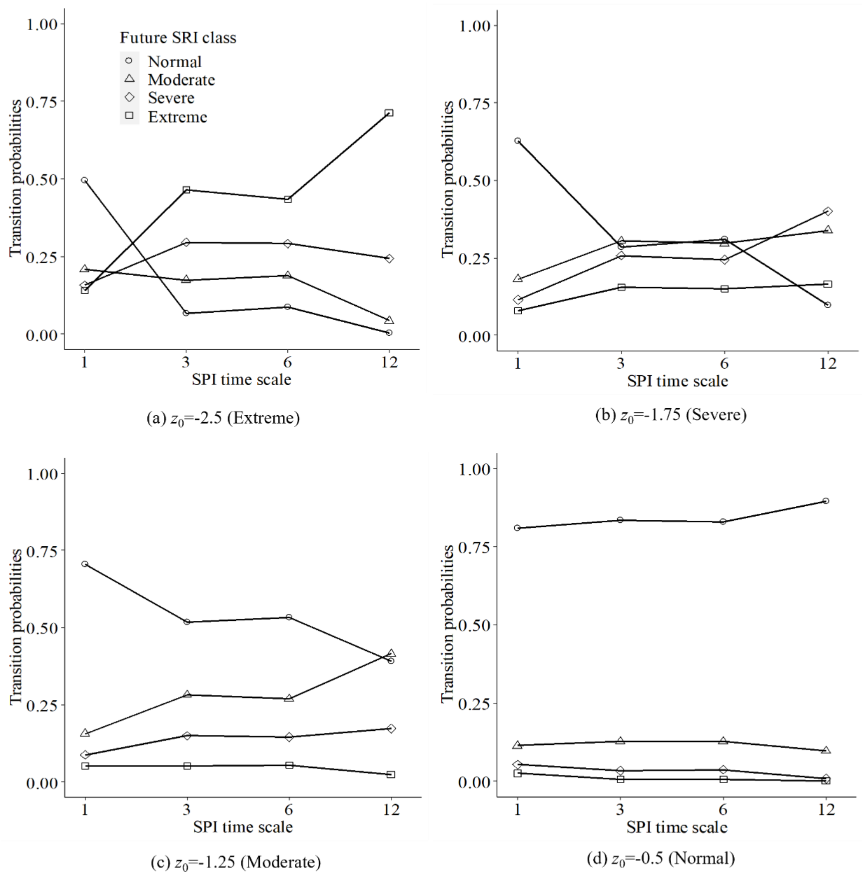

(a) z_0=-2.5 (Extreme)

(b) z_0=-1.75 (Severe)

(c) z_0=-1.25 (Moderate)

(d) z_0=-0.5 (Normal)

Figure (3). Influence of the SPI time scale on transition probabilities (z_0 : initial value of SPI)

https://doi.org/10.5194/nhess-2022-244
Preprint. Discussion started: 18 October 2022

Natural Hazards and Earth System Sciences
Open Access
Discussions

In addition, the transition probabilities of drought are distinct for different forecast periods. As seen in Figure 4(a), while the current period z_0 = -2.5, i.e., the meteorological drought is extreme drought and the forecast period is 1 and 2 months, the probability of its future SRI class being extreme drought is the highest. Moreover, the probability of its future SRI drought class returning to normal status becomes higher as the forecast period becomes longer. When the current period z_0 =-1.75 (Figure 4 (b)), namely, the meteorological drought is severe drought and the forecast period is 1 month, its future SRI class tends to be normal or moderate drought. While the forecast period becomes longer, its drought degree gradually decreases and tends to be normal. When the current period z_0 =-1.25 (Figure 4 (c)), namely, the meteorological drought is a moderate drought, the future SRI class tends to be a normal or moderate drought state as the forecast period is 1 month. In addition, its drought degree gradually decreases and tends to be normal, while the forecast period becomes longer. It is worth noting that the current z_0 =0 (Figure 4 (d)), and the probability that the future SRI class is normal as the forecast period is 1, 2 and 3 months is greater than 0.8.

https://doi.org/10.5194/nhess-2022-244
Preprint. Discussion started: 18 October 2022

Natural Hazards and Earth System Sciences
Open Access
EGU
Discussions

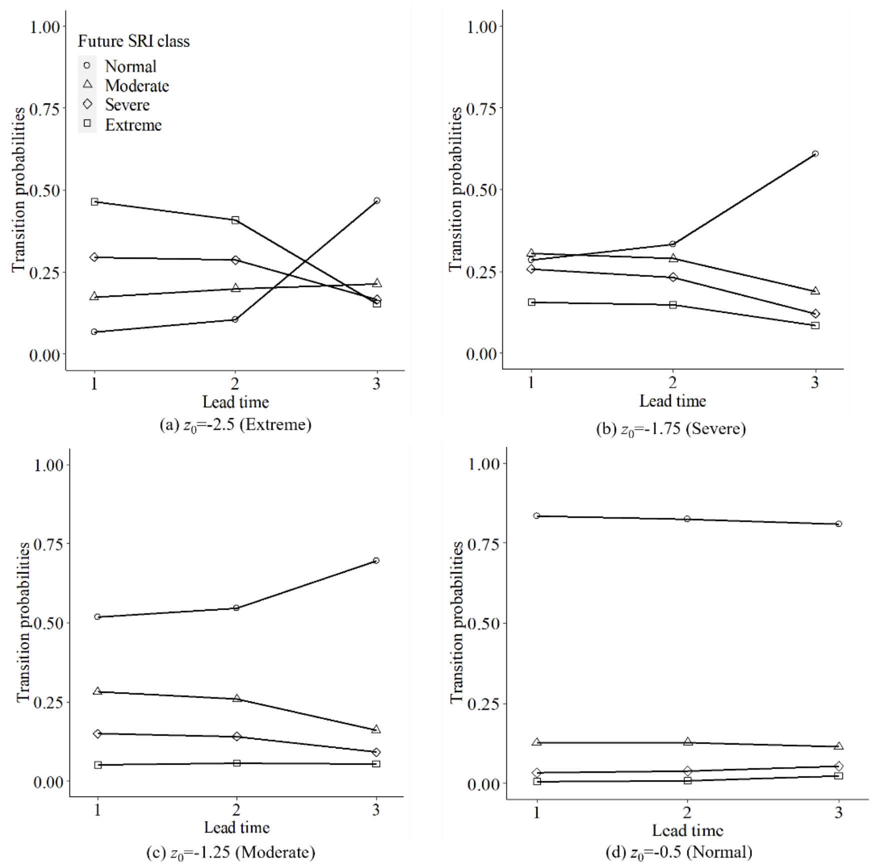

Figure (4) Influence of forecast period on transition probabilities (z_0 :initial value of SPI)

From the above analysis, when the forecast period is short (M=1 or 2), the hydrological drought class obtained from the transition of meteorological drought tends to be the same as that of meteorological drought. With the extension of the forecast period (M=2 or 3), the overall SRI class obtained from the transition tends to be slightly lower than the SPI drought class or to the normal state, i.e., the hydrological drought class obtained from the transition tends to be slightly lighter than the meteorological drought on the whole or to be maintained in the normal state.

4.3 Transition probabilities with involving *HI* as the covariate

According to the above nonstationarity test results, 1979 was the change point, and the linear regression relationship of the cumulative rainfall and runoff series

https://doi.org/10.5194/nhess-2022-244
Preprint. Discussion started: 18 October 2022

before and after the change point were established. The calculation results are shown in Table 3:

Table 3 Linear regression relationship between cumulative precipitation (x / mm) and cumulative runoff ($y/10^6\mathrm{m}^3$)

Period	Linear regression equation	Correlation coefficient
1961~1979	$x = 0.0276y + 2.7566$	0.99
1980~2010	$x = 0.0307y - 30.652$	0.98

The HI results for different time scales are shown in Figure 5.

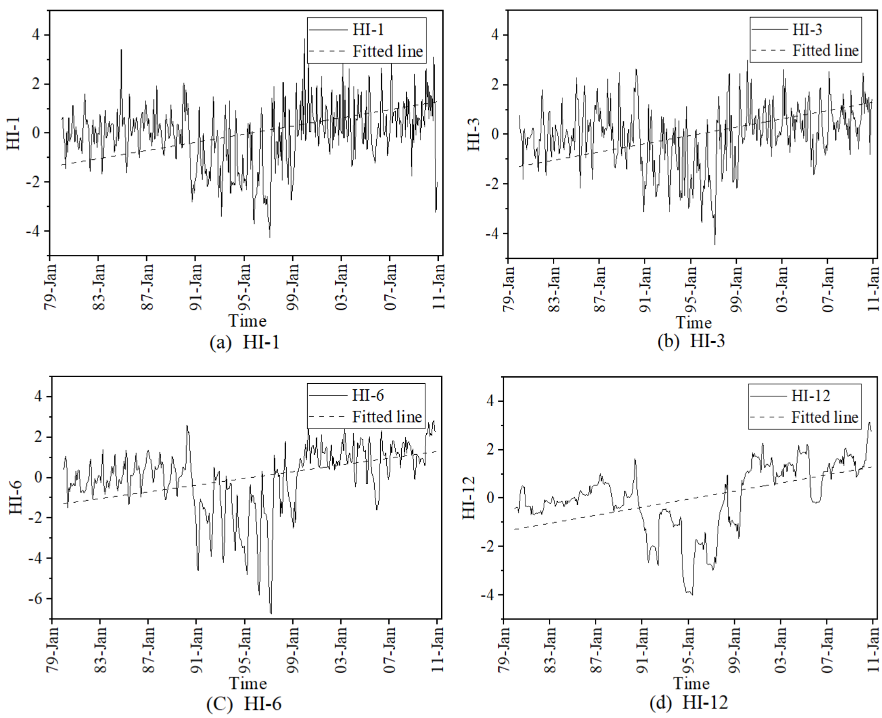

Figure 5 Different average periods of *HI* (*HI*-1: *HI* with 1-month time scale; *HI*-3: *HI* with 3-month time scale; *HI*-6: *HI* with 6-month time scale; *HI*-12: *HI* with 12-month time scale)

As shown in Figure 5, the *HI* at all monthly scales generally ranges upwards, which means that human activities have intensified the occurrence of hydrological drought.

The *HI* of different monthly scales were standardized, taking the 12-month time scale as an example, and the results were calculated as shown in Table 3.

Table 3. *HI*-12 Monthly Mean and Standard Deviation

https://doi.org/10.5194/nhess-2022-244
Preprint. Discussion started: 18 October 2022

	J	F	M	A	M	J	J	A	S	O	N	D
Mean	-0.04	-0.03	-0.03	-0.03	-0.03	0.00	0.06	0.06	0.10	0.10	0.09	0.06
Sd	1.36	1.37	1.38	1.41	1.41	1.51	1.40	1.40	1.45	1.44	1.44	1.43

Furthermore, the drought transition probabilities involving *HI* can be calculated from Eq. (23). Using the forecast period of one month from December and the SPI time scale of 12 months as an example, the drought transition probabilities from current SPI values to future SRI classes can be calculated (Figure 6). To analyse the effect of human activities on the drought transition probability more clearly, the calculation results of the three models are compared here separately. The horizontal coordinate indicates the drought classes corresponding to the SRI for the coming month, and the vertical coordinate is the drought transition probability.

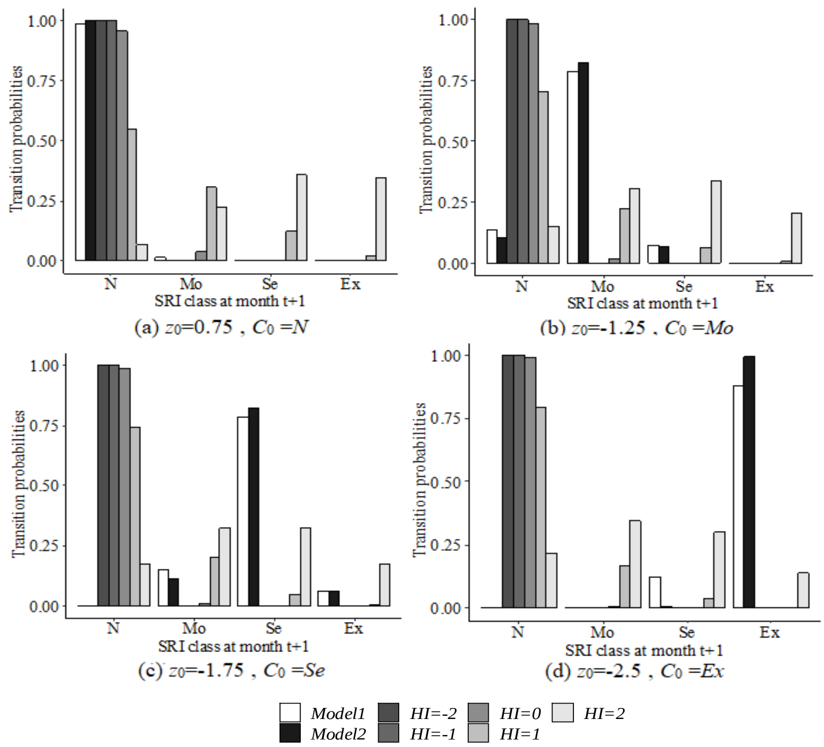

Figure 6 Drought transition probability under the influence of human activities (C_0 denotes the initial drought class of SPI in the multivariate normal model; z_0 represents the initial value of SPI in the conditional distribution model; Model 1: The normal distribution model; Model 2: The conditional distribution model; Model 3: The conditional distribution model involving *HI*)

In Figure 6 (a), when the initial z_0=0.75 and C_0=*N*, the results shown in Model 1 and Model 2 are similar, and the probability transitions of SPI values to SRI classes in the future month in the normal class are close to 1. However, the results of Model 3 indicate that the probabilities of maintaining SRI in the normal class in the future decrease as *HI* increases. When *HI*=2, the probability of transition to severe drought or extreme drought is higher.

From the initial z_0=-1.25 and C_0=*Mo* (Figure 6 (b)), it can be seen from the results of Model 3 that the transition probabilities of SPI values to a normal SRI class in the coming month are higher when *HI* is less than 1. As the *HI* increases, the transition probabilities of the SPI values to a moderate drought or even a more severe drought in the future increase. In addition, the probabilities of maintaining drought at moderate drought are the highest when human activities are not considered, and Model 2 shows a higher probability.

While the initial meteorological drought class is a severe drought (Figure 6 (c)), the probabilities of the future SRI drought class being in the normal class become larger as the *HI* decreases. When the effect of human activities is not considered, the probability that the current SPI value transitions to the SRI class under severe drought in the future month is the highest, and the probability of being in the normal class is the lowest. For Model 1, the probability of the SRI classes transitioning to a moderate drought is higher than the result of Model 2.

It is noteworthy that when the initial z_0=-2.5 and C_0=*Es* (Figure 6 (d)), the probabilities of transition of the SPI values to future SRI classes at the normal class are close to 1 as *HI*<0. However, hydrological drought is more likely to be moderate drought or severe drought as *HI* are greater than 0, and the transition probabilities exceed 0.25. For Model 1 and Model 2, the probabilities of transition of current SPI values or classes to the future month SRI classes also in extreme drought are both higher than 0.75. Model 1 shows a higher probability than Model 2 when the SRI class transitions to severe drought.

https://doi.org/10.5194/nhess-2022-244
Preprint. Discussion started: 18 October 2022

4.4 Model evaluation and analysis

To quantitatively evaluate the prediction accuracy of Model 1, Model 2 and Model 3, the study period is divided into a correction period (1961-2003) and a verification period (2004-2010), and then the drought transition probability from the SPI value or class to the SRI class in the future M-month is calculated. The monthly drought transition probability is summed to evaluate the model (Chen et al., 2013):

$$Score = \frac{1}{12n}\sum_{t=1}^{12}\sum_{s=1}^{n} p_{s,t} \tag{29}$$

where $p_{s,t}$ characterizes the transition probability in month t of year s, and n is the length of the validation period. The calculation results are shown in Table 5.

With the same time scale of SPI, the model scores of Model 1 and Model 2 lowers as the forecast period *M* lengthens, while the model scores of Model 3 are not significantly affected by the forecast period *M*. Model 1 had the highest rating of 0.36 at an SPI of 1-month time scale and a forecast period of one month; Model 2 reached the highest model rating of 0.74 at a 12-month time scale and a forecast period of one month; and model-3 performed well at an SPI of 1-month time scale and a 12-month time scale. Overall, model-3 has the highest rating, and Model 1 has the lowest rating for the same SPI time scale and the same forecast period, which also indicates that the forecast accuracy of the conditional distribution model considering the *HI* is higher for short-term forecasts with a forecast period of 3 months or less, and involving the *HI* can further improve the forecast accuracy of the model.

Table 5. Model Evaluation (Model 1: Multivariate normal distribution model; Model 2: Conditional distribution model; Model 3: Conditional distribution model with *HI*)

Model type	Lead time *M*	SPI time scale			
		1	3	6	12
Model 1	1	0.36	0.36	0.28	0.22
	2	0.11	0.35	0.27	0.22
	3	0.02	0.34	0.26	0.22
Model 2	1	0.69	0.52	/	0.74
	2	0.69	0.47	/	0.67
	3	0.69	0.44	0.39	0.60

https://doi.org/10.5194/nhess-2022-244
Preprint. Discussion started: 18 October 2022

Natural Hazards and Earth System Sciences
Open Access
Discussions

Model 3	1	0.72	0.64	0.59	0.71
	2	0.71	0.64	0.59	0.71
	3	0.72	0.64	0.60	0.71

5 Conclusions

Many studies have pointed out that human activities have a significant impact on watershed runoff in the Luanhe River Basin. In this paper, three probability models were constructed to calculate the transition probabilities from current SPI classes or values to future SRI classes; then, a scoring mechanism was applied to evaluate the performance of the models.

Under the condition of considering the *HI*, the calculation results of the drought transition probability show that when the value of *HI* is less than 0, human activity slows the occurrence of hydrological drought and the probability of maintaining hydrological drought at the normal class peaks. With the increase in the *HI* value, it is easier for hydrological droughts to transition to more severe droughts. The calculation results of Model 1 and Model 2 show that the future hydrological drought classes are likely to be the same as the meteorological drought classes in the current period.

Finally, a scoring mechanism was applied to the evaluation of the models, and the forecast results of the three models were evaluated. The results demonstrate that when the SPI time scale is the same, the scores of Model 1 and Model 2 lower as the forecast period lengthens. In most cases, Model 2 performs better than Model 1, and the performance of Model 3 is the most stable of the three models and has the highest score. In addition, the performance of Model 3 is not affected by the forecasting period. The conditional probability model considering *HI* is more suitable for the Luanhe River basin, where human activities have a high influence.

Although this study has made some progress in the forecasting of hydrological drought in the changing environment, only one exogenous variable was calculated to quantify the impact of human activities, and the climate factors can be further considered in future studies. In addition, *HI* can be analysed specifically, such as land use and social economy.

Limitation: Under changing environmental conditions, the driving factors of drought can be analysed from the physical mechanism, such as considering the influence of large-scale climate indices or hydro-meteorological variables, to further improve the forecasting accuracy of hydrological drought.

Ethical Approval: This work meets the ethical and moral requirements.

Consent to Participate: M L. MF Z. RX C. YD S and XY D all agreed to participate in the research for the article.

Consent to Publish: M L. MF Z. RX C. YD S and XY D all agreed to publish this article.

Authors Contributions:

M L(First Author and Corresponding Author)：Conceptualization, Methodology, Software, Investigation, Formal Analysis, Writing-Original Draft;

MF Z：Data Curation, Writing-Original Draft;

RX C: Visualization, Investigation;

YD S: Resources, Supervision;

XY D: Visualization, Writing-Review & Editing.

Competing interest: M L. MF Z. RX C. YD S and XY D all declare that there is no conflict of interest.

Data availability statement: We are grateful to the Hydrology and Water Resource Survey Bureau of Hebei Province for providing runoff data. The data and materials of the research are available.

References

[1] Abbasi Abbas,Khalili Keivan,Behmanesh Javad,Shirzad Akbar. Estimation of ARIMA model parameters for drought prediction using the genetic algorithm[J]. Arabian Journal of Geosciences,2021,14(10): 841-841.

[2] Ahnadi mahmoud. Climatic drought forecasting using artificial neural network in Hamedan region[J]. New York Science Journal,2011,4(8):15-19.

[3] Alquraish Mohammed,Ali. Abuhasel Khaled,S. Alqahtani Abdulrahman,Khadr Mosaad. SPI-Based Hybrid Hidden Markov–GA, ARIMA–GA, and ARIMA–GA–ANN Models for Meteorological Drought Forecasting[J]. Sustainability,2021,13(22): 12576-12576.

[4] Bagher Shirmohammadi,Hamidreza Moradi,Vahid Moosavi,Majid Taie Semiromi,Ali Zeinali. Forecasting of meteorological drought using Wavelet-ANFIS hybrid model for different time steps (case study: southeastern part of east Azerbaijan province, Iran)[J]. Natural Hazards,2013,69(1): 389-402.

[5] Behzad Ahmadi,Hamid Moradkhani. Revisiting hydrological drought propagation and recovery considering water quantity and quality[J]. Hydrological Processes,2019,33(10):1492-1505.

[6] Bishara Anthony J,Hittner James B. Testing the significance of a correlation with nonnormal data: comparison of Pearson, Spearman, transformation, and resampling approaches.[J]. Psychological methods,2012,17(3):399-417.

[7] Bonaccorso B, Cancelliere A, Rossi G. Probabilistic forecasting of drought class transitions in Sicily (Italy) using Standardized Precipitation Index and North Atlantic Oscillation Index[J]. Journal of Hydrology, 2015, 526: 136-150.

[8] Carmelo Cammalleri,Jürgen V. Vogt. Non-stationarity in MODIS fAPAR time-series and its impact on operational drought detection[J]. International Journal of Remote Sensing,2018,40(4):1428-1444.

[9] Chang Guobin, Zhang Shubi, Liu Zhiping. Understanding the adjusment from an information theoretic perspective[J/OL]. Geomatics and Information Science of Wuhan University:1-17[2022-03-07]. (in Chinese)

[10] Charles Onyutha. On Rigorous Drought Assessment Using Daily Time Scale: Non-Stationary Frequency Analyses, Revisited Concepts, and a New Method to Yield Non-Parametric Indices[J]. Hydrology,2017,4(4): 48-48.

[11] Chen Jie, Brissette François P, Chaumont Diane, Braun Marco. Performance and uncertainty evaluation of empirical downscaling methods in quantifying the climate change impacts on hydrology over two North American river basins[J]. Journal of Hydrology,2013,479: 200-214.

[12] Ding Yibo,Xu Jiatun,Wang Xiaowen,Cai Huanjie,Zhou Zhaoqiang,Sun Yanan,Shi Haiyun. Propagation of meteorological to hydrological drought for different climate regions in China[J]. Journal of Environmental Management,2021,283: 111980-111980.

[13] Dixit, Soumyashree,Jayakumar, K. V.. A Non-stationary and Probabilistic Approach for Drought Characterization Using Trivariate and Pairwise Copula Construction (PCC) Model[J]. Water Resources

https://doi.org/10.5194/nhess-2022-244
Preprint. Discussion started: 18 October 2022

Management,2022(prepublish): 1-20.

[14] Fuentes Ignacio,Padarian José,Vervoort R. Willem. Spatial and Temporal Global Patterns of Drought Propagation[J]. Frontiers in Environmental Science,2022:788248-788248.

[15] Gang Zhao,Huilin Gao,Shih-Chieh Kao,Nathalie Voisin,Bibi S. Naz. A modeling framework for evaluating the drought resilience of a surface water supply system under non-stationarity[J]. Journal of Hydrology,2018,563: 22-32.

[16] Gong Haonan, Xie Botao, Wang Junrong, et al. Long-term prediction of extreme response of deepwater floating platform based on environmental contour method[J]. The Ocean Engineering,2021,39(05):28-38. (in Chinese)

[17] Kolachian Roya,Saghafian Bahram. Hydrological drought class early warning using support vector machines and rough sets[J]. Environmental Earth Sciences,2021,80(11):390-390.

[18] Koudahe K,Koffi D,Kayode JA,Awokola SO,Adebola AA. Impact of Climate Variability on Crop Yields in Southern Togo[J]. Environment Pollution and Climate Change,2018,2(1): 1-9.

[19] Li Jianzhu, Wang Y X, Li S F, Hu R. Hu. A Nonstationary Standardized Precipitation Index incorporating climate indices as covariates[J]. Journal of Geophysical Research: Atmospheres,2015,120(23):082-095.

[20] Li Linchao, Yao Ning, Li Yi, Liu De Li, Wang Bin, Ayantobo Olusola O. Future projections of extreme temperature events in different sub-regions of China[J]. Atmospheric Research,2018,217:150-164.

[21] Li Xin,Fang Guohua,Wen Xin,Xu Ming,Zhang Yu. Characteristics analysis of drought at multiple spatiotemporal scale and assessment of CMIP6 performance over the Huaihe River Basin[J]. Journal of Hydrology: Regional Studies,2022,41:101-103.

[22] Li Xinxin,Ma Xixia,Li Xiaodong,Zhang Wenjiang. Method Consideration of Variation Diagnosis and Design Value Calculation of Flood Sequence in Yiluo River Basin, China[J]. Water,2020,12(10): 2722-2722.

[23] Malede Demelash Ademe,Agumassie Tena Alamirew,Kosgei Job Rotich,Linh Nguyen Thi Thuy,Andualem Tesfa Gebrie. Analysis of rainfall and streamflow trend and variability over Birr River watershed, Abbay basin, Ethiopia[J]. Environmental Challenges,2022,7:100528-100528.

[24] Mallya G,Tripathi S,Kirshner S,Rao S. Govindaraju. Probabilistic Assessment of Drought Characteristics Using Hidden Markov Model[J]. Journal of Hydrologic Engineering,2013,18(7): 834-845.

https://doi.org/10.5194/nhess-2022-244
Preprint. Discussion started: 18 October 2022

[25] Maryam Mokhtarzad,Farzad Eskandari,Nima Jamshidi Vanjani,Alireza Arabasadi. Drought forecasting by ANN, ANFIS, and SVM and comparison of the models[J]. Environmental Earth Sciences,2017,76(21): 729-729.

[26] McKee, T.B., Doesken, N.J., Kleist, J.The relationship of drought frequency and duration to time scales. In: Proc. 8th Conference on Applied Climatology, Anaheim, California, 1993: 179–184.

[27] Mehdi Rezaeianzadeh,Alfred Stein,Jonathan Peter Cox. Drought Forecasting using Markov Chain Model and Artificial Neural Networks[J]. Water Resources Management,2016,30(7): 2245-2259.

[28] Melanie Oertel,Francisco Javier Meza,Jorge Gironás,Christopher A. Scott,Facundo Rojas,Nicolás Pineda-Pablos. Drought Propagation in Semi-Arid River Basins in Latin America: Lessons from Mexico to the Southern Cone[J]. Water,2018,10(11): 1564-1564.

[29] Miriam Fendeková,Tobias Gauster,Lívia Labudová,Dana Vrablíková,Zuzana Danáčová,Marián Fendek,Pavla Pekárová. Analysing 21st century meteorological and hydrological drought events in Slovakia[J]. Journal of Hydrology and Hydromechanics,2018,66(4): 393-403.

[30] Mohammad Mehdi Moghimi,Abdol Rassoul Zarei,Mohammad Reza Mahmoudi. Seasonal drought forecasting in arid regions, using different time series models and RDI index[J]. Journal of Water and Climate Change,2020,11(3): 633-654.

[31] Moreira Elsa E,Mexia João T.,Pereira Luís S. Assessing homogeneous regions relative to drought class transitions using an ANOVA-like inference. Application to Alentejo, Portugal[J]. Stochastic Environmental Research and Risk Assessment,2013,27(1): 183-193.

[32] Muhammad Jehanzaib,Sabab Ali Shah,Jiyoung Yoo,Tae-Woong Kim. Investigating the impacts of climate change and human activities on hydrological drought using non-stationary approaches[J]. Journal of Hydrology,2020,588:125052-125052.

[33] Natsagdorj Enkhjargal,Renchin Tsolmon,Maeyer Philippe De,Darkhijav Bayanjargal. Spatial Distribution of Soil Moisture in Mongolia Using SMAP and MODIS Satellite Data: A Time Series Model (2010–2025)[J]. Remote Sensing,2021,13(3): 347-347.

[34] Palmer, W.C., 1965. Meteorological Drought, Research Paper, 45, U.S. Weather Bureau.

[35] Ren Weinan, Wang Yixuan, Li Jianzhu , Feng Ping, Smith Ronald J. Drought forecasting in Luanhe River basin involving climatic indices[J]. Theoretical and Applied Climatology,2017,130(3-4): 1133-1148.

https://doi.org/10.5194/nhess-2022-244
Preprint. Discussion started: 18 October 2022

[36] Shraddhanand Shukla and Andrew W. Wood. Use of a standardized runoff index for characterizing hydrologic drought[J]. Geophysical Research Letters, 2008, 35(2): 2405-1-2405-7.

[37] Stojković Milan,Plavšić Jasna,Prohaska Stevan,Pavlović Dragutin,Despotović Jovan. A two-stage time series model for monthly hydrological projections under climate change in the Lim River basin (southeast Europe)[J]. Hydrological Sciences Journal,2020,65(3): 387-400.

[38] Wang Menghao,Jiang Shanhu,Ren Liliang,Xu Chong-Yu,Menzel Lucas,Yuan Fei,Xu Qin,Liu Yi,Yang Xiaoli. Separating the effects of climate change and human activities on drought propagation via a natural and human-impacted catchment comparison method[J]. Journal of Hydrology,2021,603(PA):126913-123613.

[39] Wang Yixuan, Duan Limin, Liu Tingxi, Li Jianzhu, Feng Ping. A Non-stationary Standardized Streamflow Index for hydrological drought using climate and human-induced indices as covariates[J]. Science of the Total Environment,2020,699(C):134278-134278.

[40] Wang Yixuan, Li Jianzhu , Feng Ping, Hu Rong. Analysis of drought characteristics over Luanhe River basin using the joint deficit index[J]. Journal of Water and Climate Change,2016,7(2): 340-352.

[41] Wang Yixuan, Zhang Ting, Chen Xu, Li Jianzhu, Feng Ping. Spatial and temporal characteristics of droughts in Luanhe River basin, China[J]. Theoretical and Applied Climatology,2018,131(3): 1369-1385.

[42] Wang Youxin,Peng Tao,Lin Qingxia,Singh Vijay P.,Dong Xiaohua,Chen Chen,Liu Ji,Chang Wenjuan,Wang Gaoxu. A New Non-stationary Hydrological Drought Index Encompassing Climate Indices and Modified Reservoir Index as Covariates[J]. Water Resources Management,2022,36(7): 2433-2454.

[43] Wu Huizhuo. A Sufficient Condition for Determining the Normal Distribution of Two-dimensional Random Variables[J]. College Mathematics,2019,35(06): 63-65. (in Chinese)

[44] Xu Yang, Zhang Xuan, Wang Xiao, Hao Zengchao, Singh Vijay P, Hao Fanghua. Propagation from meteorological drought to hydrological drought under the impact of human activities: A case study in northern China[J]. Journal of Hydrology,2019,579(C): 124147-124147.

[45] Yixuan Wang,Jianzhu Li,Ping Feng,Fulong Chen. Effects of large-scale climate patterns and human activities on hydrological drought: a case study in the Luanhe River basin, China[J]. Natural Hazards,2015,76(3): 1687-1710.

[46] Zhang Ting et al. Drought class transition analysis through different models: a case study in North

China[J]. Water Science & Technology: Water Supply, 2017, 17(1): 138-150.

[47] Aghelpour Pouya and Varshavian Vahid. Forecasting Different Types of Droughts Simultaneously Using Multivariate Standardized Precipitation Index (MSPI), MLP Neural Network, and Imperialistic Competitive Algorithm (ICA)[J]. COMPLEXITY, 2021, 2021

[48] Majid Dehghani, Bahram Saghafian and Mansoor Zargar. Probabilistic hydrological drought index forecasting based on meteorological drought index using Archimedean copulas[J]. Hydrology Research, 2019, 50(5) : 1230-1250.

Acknowledgements: This work was supported by the State Key Laboratory of Hydraulic Engineering Simulation and Safety Program (No. HESS-2206 and No. HESS-2222).